Mapping Concurrent Spatiotemporal Trends of Drought Conditions and Dust Occurrence across Iran Using Long-Term Satellite and Climate Data

Masoud Soleimani[1], Ali Darvishi Boloorani[1,*], Najmeh Neysani Samany[1], Mohammad Reza Ghayamghamian[2], Ali Al-Hemoud[3]

1- Department of Remote Sensing and GIS, Faculty of Geography, University of Tehran, Tehran, Iran.
2- International Institute of Earthquake Engineering and Seismology, Risk Management Research Center, Tehran, Iran.
3- Environment and Life Sciences Research Center, Kuwait Institute for Scientific Research, Kuwait City, Kuwait.

***Corresponding Author:** ali.darvishi@ut.ac.ir

Abstract
Drought and dust are major environmental hazards affecting Iran, yet their long-term spatial concurrence remains insufficiently characterized. This study investigates the spatiotemporal patterns and concurrent trends of drought and dust occurrence across Iran during 2000–2024 using daily MODIS MAIAC aerosol optical depth (AOD) observations and monthly TerraClimate Palmer Drought Severity Index (PDSI) data. Long-term trends in dust frequency and drought conditions were assessed using Sen's slope and the Mann–Kendall test. Dust occurrence showed strong spatial heterogeneity, with predominantly increasing trends, particularly across central, eastern, and northeastern Iran. Drought conditions were similarly heterogeneous, with increasing trends concentrated mainly in eastern and southeastern regions. Integrated analysis revealed that concurrent increases in drought conditions and dust events covered 17% of Iran, while increasing drought conditions accompanied by non-significant dust trends formed the largest class (24%). Concurrent decreases were negligible (<1%). These findings highlight substantial regional differences in drought–dust dynamics and demonstrate the value of an integrated trend-based framework for identifying areas where drought and dust trends occur concurrently under climate change.

Keywords: Climate Change, Palmer Drought Severity Index (PDSI), Aerosol Optical Depth (AOD), Trend Analysis, Dust Frequency.

Introduction
Climate change is increasingly altering hydroclimatic conditions across many regions of the world, with particularly pronounced consequences in arid and semi-arid environments (Zittis et al., 2022). The Middle East is widely recognized as highly exposed to climate-related changes, where rising temperatures, shifting precipitation patterns, and intensifying hydroclimatic stress are already affecting water resources, ecosystems, and human societies (Darvishi Boloorani et al., 2024a). Recent assessments indicate that drought conditions have intensified across several arid and semi-arid regions (Darvishi Boloorani et al., 2026a), and the combination of warming, drying, vegetation loss, land degradation, and the desiccation of water bodies can increase the susceptibility of dryland surfaces to aeolian processes and dust emissions (Neira et al., 2023; IPCC, 2023; Darvishi Boloorani et al., 2024b).
Iran is particularly vulnerable to the concurrent occurrence of drought (Tosan et al., 2025) and atmospheric dust because of its predominantly arid and semi-arid climate, extensive drylands, and location within the global dust belt (Ginoux et al., 2012; Shi et al., 2021). Approximately 93% of Iran is classified as arid, semi-arid, or hyper-arid, providing extensive areas susceptible to dust emission (Rashki et al., 2021). Dust storms represent a persistent environmental hazard in Iran, with well-documented implications for human health and socioeconomic activities, agricultural production, forest ecosystems, energy production, industry, and infrastructure (Rashki et al., 2021; Pato et al., 2025; MalAmiri et al., 2025).

Pre-publication Version

Dust affecting Iran originates from both domestic and transboundary sources. Important external source regions include the deserts and alluvial plains of Iraq and Syria, while substantial internal sources are distributed across western, southwestern, eastern, and central Iran (Rashki et al., 2021). The environmental controls of dust emission are multifaceted, involving wind speed and direction, soil properties, surface moisture, vegetation cover, land degradation, surface roughness, and the availability of exposed sediment (Sotoudeheian et al., 2016). Within this framework, drought can contribute to conditions favorable for dust emission through reduced precipitation and soil moisture, vegetation degradation, and the desiccation of wetlands and other surface-water bodies (Ahrari et al., 2024). Evidence from central Iran has shown that severe drought conditions can intensify the frequency of dust emissions from different types of potential dust-source areas (Papi et al., 2022). More recently, a basin-scale assessment of the Tigris–Euphrates Basin found that dust-event occurrence increased substantially during drought periods, with the two major drought episodes of 2008–2012 and 2021–2022 associated with increases of approximately 214% and 200%, respectively, relative to the long-term average (Darvishi Boloorani et al., 2024c). These findings demonstrate that drought and dust are closely connected environmental hazards in the region, although their relationship is spatially heterogeneous and influenced by multiple climatic, surface, and anthropogenic factors.

Understanding the spatiotemporal co-evolution of drought and dust occurrence is therefore important for assessing environmental vulnerability and for supporting climate adaptation and land management strategies in Iran. The country provides a particularly suitable setting for such a nationwide assessment because of its diverse climatic regimes, extensive and spatially heterogeneous dust source areas, and substantial regional variability in drought conditions. Drought monitoring has been extensively supported by meteorological observations, remote sensing products, and gridded climate datasets, with previous studies documenting substantial spatiotemporal variability in drought severity across different climatic regions (Pouyan et al., 2023; Rahnama et al., 2024; Fakhar et al., 2024; Mahdizadeh et al., 2025). Previous studies have also substantially improved knowledge of dust sources, transport pathways, seasonal variability, and climatic controls across different parts of the country (Darvishi Boloorani et al., 2026b). Satellite observations have further provided valuable opportunities for monitoring long-term aerosol and dust variability over areas where ground-based observations are spatially limited (Soleimani et al., 2021). For example, MODIS-based studies have identified substantial spatial heterogeneity in aerosol loading and dust activity across Iran (Soleimani et al., 2026). However, much of the existing literature has focused on individual regions, specific dust events, individual climatic drivers, or separate assessments of drought and dust variability. A consistent national-scale framework that simultaneously characterizes long-term trends in drought conditions and dust occurrence and explicitly examines their spatial concurrence remains comparatively limited. This is particularly relevant because spatially aggregated relationships may conceal substantial regional differences in the direction and magnitude of trends.

Against this background, this study aims to investigate the concurrent spatiotemporal trends of drought and dust occurrence across Iran over the period 2000–2024. The study seeks to provide a comprehensive national-scale assessment of how these two environmentally important hazards have evolved over the past few decades and, more importantly, to identify areas where their trends occur concurrently, in contrasting directions, or where a significant trend in one variable is not accompanied by a significant trend in the other. By integrating long-term environmental observations with spatiotemporal trend analysis, the study provides a spatially explicit characterization of drought–dust dynamics across Iran. The findings are expected to improve the understanding of the spatial heterogeneity of drought and dust patterns in Iran and provide a broader evidence base for environmental vulnerability assessment, climate change adaptation, and sustainable land and environmental management.

Materials and Methods

Methodological Framework

This study employs an integrated geospatial framework to investigate the concurrent trends of drought and dust occurrence across Iran during 2000–2024 (Fig. 1). The methodological framework combines long-term satellite-based aerosol observations with gridded climate data to characterize the temporal behavior

Pre-publication Version

and spatial distribution of the two environmental hazards. First, daily Aerosol Optical Depth (AOD) observations from the MODIS Terra and Aqua platforms are processed to derive a spatially explicit Dust Frequency Indicator (DFI), while monthly Palmer Drought Severity Index (PDSI) data from TerraClimate are used to characterize drought conditions over the study period. The temporal trends of both indicators are subsequently evaluated at the pixel level and classified according to their direction and statistical significance. The resulting trend maps are then integrated within a Geographic Information System (GIS) environment using a spatial overlay approach to identify areas characterized by different combinations of drought and dust trends. The final spatial classification provides a national-scale representation of the concurrent evolution of the two hazards and enables the identification of areas where increasing or decreasing trends occur simultaneously. Overall, this framework is designed to reveal the spatial heterogeneity of drought–dust dynamics across Iran and provide an integrated basis for their spatial characterization and interpretation.

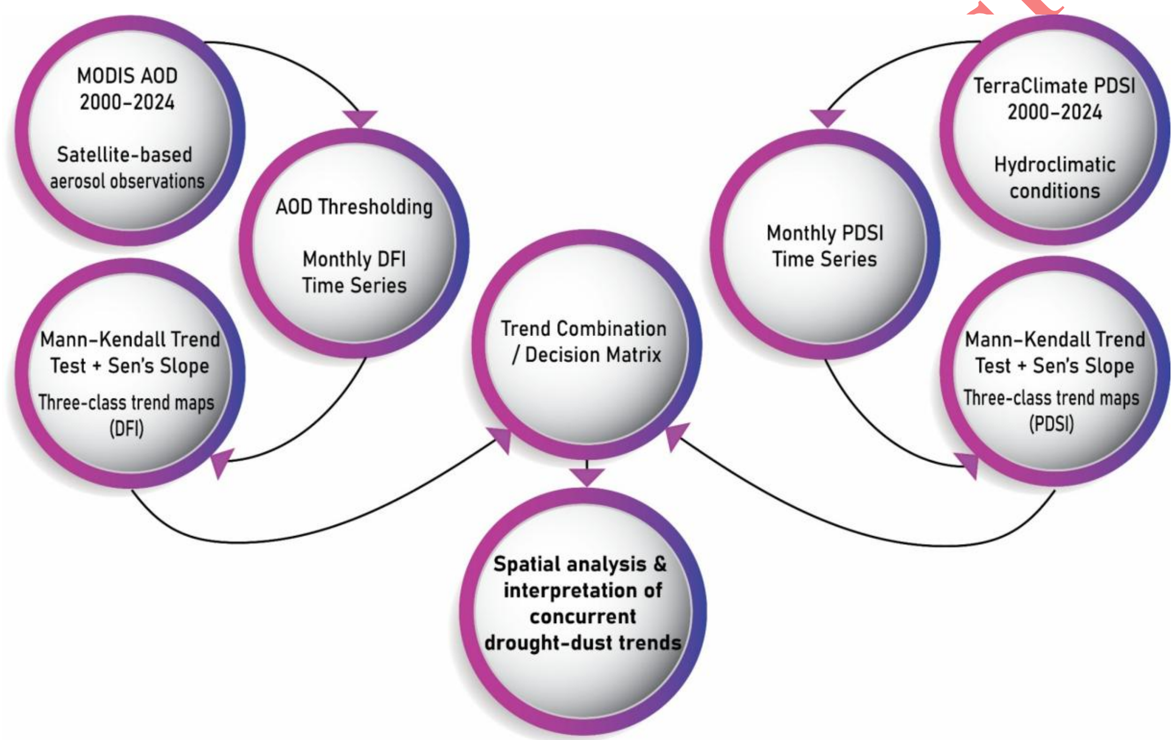

Fig 1. Schematic workflow of the methodological framework used to assess the concurrent spatiotemporal trends of drought and dust occurrence across Iran during 2000–2024.

Study Area

Iran is located in West Asia between approximately 25°–40° N and 44°–63° E, covering an area of about 1.65 million km^2 (Fig. 2). The country is characterized by pronounced climatic, topographic, and environmental heterogeneity, ranging from humid and temperate conditions along the Caspian Sea in the north to extensive arid and semi-arid landscapes across central, eastern, southern, and southwestern regions (Mesgaran et al., 2016; Eskandari Dameneh et al., 2021). Large parts of Iran are occupied by deserts and drylands, including the Kavir Desert and Lut Desert, which, together with degraded lands, dry lakebeds, wetlands, and sparsely vegetated surfaces, provide favorable conditions for dust emission (Rashki et al., 2021; Papi et al., 2022; Ahrari et al., 2024). The country's complex topography is dominated by two major mountain systems, the Alborz Mountains in the north and the Zagros Mountains extending from the northwest toward the south and southwest. These mountain ranges strongly influence regional atmospheric circulation, precipitation distribution, and the transport pathways of airborne aerosols and dust (Vaghefi et al., 2019).

Iran is influenced by both domestic and transboundary sources of mineral dust, with important source regions occurring within the country as well as across neighboring drylands, particularly in Iraq and the broader Mesopotamian region (Soleimani et al., 2026). To provide a clearer spatial context for the distribution of dust activity across Iran, main dust source areas were identified through visual interpretation of daily MODIS Terra and Aqua true-color imagery available through NASA's EOSDIS Worldview platform (Al-Hemoud et al., 2024). The interpretation covered the 2000–2024 period and focused on the recurrent emergence of visible dust plumes from exposed, sparsely vegetated, and dry surfaces and their subsequent development and movement across the landscape. Areas showing recurrent plume initiation from identifiable exposed surfaces were distinguished from areas where dust was primarily observed as transported plumes without a consistent connection to an identifiable surface source. The identified areas were considered representative of the major regions associated with frequent dust activity and were delineated and displayed on the study area map (Fig. 2). These source regions are generally characterized by recurrent dust emission and, under favorable atmospheric conditions, can affect surrounding and downwind areas through regional dust transport (Darvishi Boloorani et al., 2026b). The spatial extent and direction of such impacts are strongly influenced by prevailing wind patterns and atmospheric circulation, including the Shamal circulation affecting western and southwestern Iran and the Levar wind system influencing eastern Iran (Yu et al., 2016; Rashki et al., 2021). The mapped source areas therefore provide an important geographical context for interpreting the spatial distribution of dust occurrence and its long-term trends across the country.

Version

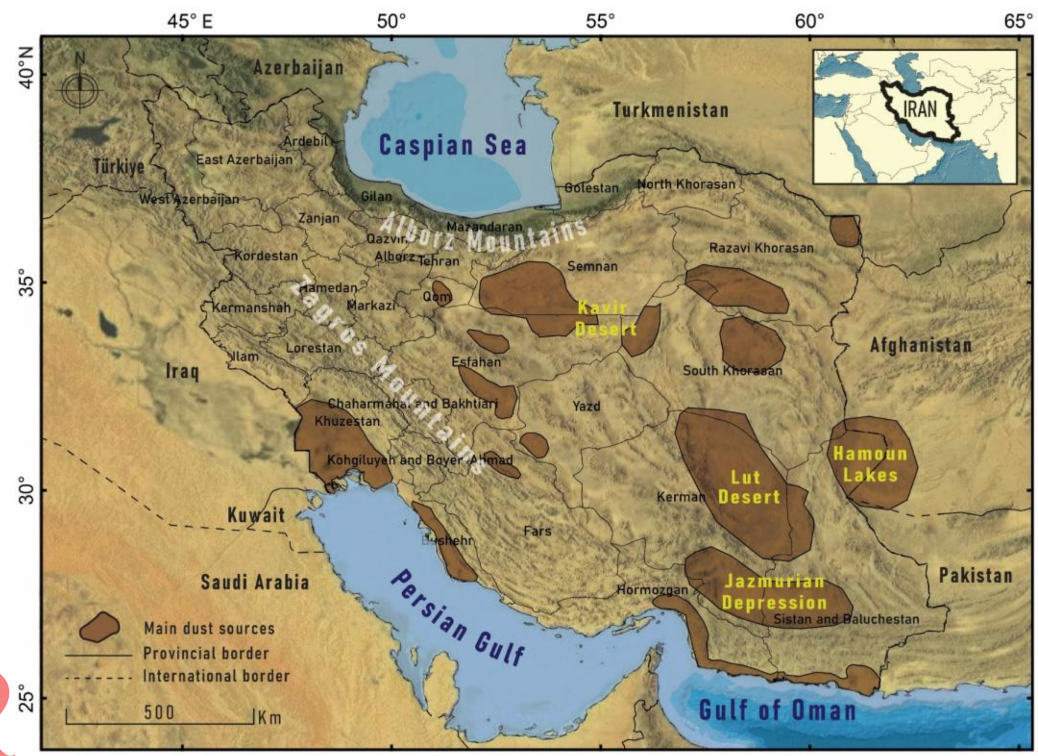

P

Fig 2. Geographical setting of Iran showing provincial boundaries, major mountain ranges, and main dust source areas identified through visual interpretation of MODIS Terra and Aqua true-color imagery during 2000–2024.

Data Sources and Preparation

The datasets required to derive the dust and drought indicators were accessed and processed through the Google Earth Engine (GEE) cloud-based geospatial computing platform. The dust and drought indicators were first analyzed independently at their respective native spatial resolutions over the common 2000–2024 study period, selected based on the availability of MODIS AOD data from 2000 onward. Pixel-wise long-term trends were then derived separately for the DFI and PDSI. Following the independent trend analyses, the resulting DFI trend map was resampled from its native 1-km spatial resolution to approximately 4 km to match the spatial resolution of the PDSI trend map. Bilinear resampling was used for this spatial matching prior to the final GIS-based integration of the two trend layers. This procedure ensured that the two trend maps were represented on a common spatial grid for the integrated drought–dust trend classification.

MODIS AOD and Dust Occurrence

Daily AOD observations were obtained from the MODIS Terra and Aqua Multi-Angle Implementation of Atmospheric Correction (MAIAC) Land Aerosol Optical Depth product (MCD19A2, Version 6.1) for the period 2000–2024. The MCD19A2 product is a daily Level-2 gridded dataset generated using the MAIAC algorithm and provides AOD at a spatial resolution of 1 km on the MODIS sinusoidal grid. The product integrates observations from the Terra and Aqua platforms and provides AOD retrievals at 0.47 and 0.55 µm, together with associated quality information and other atmospheric parameters (Lyapustin et al., 2018). In this study, AOD at 0.47 µm was used as the primary indicator of atmospheric aerosol loading. The daily observations were spatially processed over the Iranian territory to construct a pixel-level time series of AOD for subsequent identification of dusty conditions.

To distinguish dust-related aerosol loading from other atmospheric aerosol conditions, an empirical AOD threshold previously established by Soleimani et al. (2026) was adopted. In that study, the threshold was derived using a reference dataset of confirmed dust events identified through visual interpretation of daily MODIS-Terra/Aqua true-color imagery across major dust-affected regions of Iran and the Tigris–Euphrates Basin. Based on the statistical distribution of AOD values associated with the reference dust events, an AOD value of 0.39 was identified as an appropriate empirical threshold for detecting dust occurrence (Soleimani et al., 2026). Accordingly, in the present study, a pixel was classified as exhibiting dust occurrence on a given day when AOD ≥ 0.39. This binary daily classification was subsequently used to derive the DFI at the pixel level.

The DFI represents the frequency of dusty conditions at each pixel and was calculated on a monthly basis by counting the number of valid observation days classified as dusty within each calendar month (Eq. 1).

$$DFI_m = \sum_{d=1}^{D_m} I(AOD_d \geq T) \quad (1)$$

where DFI_m is the Dust Frequency Indicator for month? m, AOD_d is the AOD value on day d, T is the empirical dust-related AOD threshold, D_m is the number of days in the month m, and $I(.)$ is the indicator function, taking a value of 1 when the specified condition is satisfied and 0 otherwise. DFI was calculated only from valid MODIS AOD observations, while days with unavailable or invalid AOD data were excluded from the count. Thus, DFI provides a spatially explicit measure of the monthly recurrence of dust occurrence across Iran during the 2000–2024 study period. Higher DFI values indicate a greater frequency of dust occurrence within a given month, whereas lower values indicate less frequent dusty conditions. The resulting monthly DFI dataset was subsequently used to characterize the long-term temporal trends in dust occurrence and to assess their spatial concurrence with drought trends.

TerraClimate PDSI

Monthly PDSI data were obtained from the TerraClimate dataset for the period 2000–2024. TerraClimate is a high-resolution gridded climate dataset that provides monthly climate and climatic water-balance variables across global terrestrial surfaces at a spatial resolution of approximately 4 km. The dataset is developed using a climatically aided interpolation approach that combines spatially detailed climatological information with time-varying climate observations and reanalysis-based data, allowing the generation of spatially continuous monthly climate fields over regions with limited observational coverage (Abatzoglou et al., 2018).

The PDSI variable in TerraClimate was selected as the drought indicator because it provides a standardized measure of relative wetness and dryness based on the climatic water balance. PDSI integrates precipitation

Pre-publication Version

and temperature information with soil water balance characteristics to represent the cumulative departure of moisture conditions from locally expected conditions. Negative PDSI values indicate relatively dry conditions, with increasingly negative values representing greater drought severity, whereas positive values indicate relatively wet conditions (Abatzoglou et al., 2018). In the present study, monthly PDSI data were extracted for the Iranian territory and organized into a continuous pixel-level time series for the study period. Because the objective of this study is to characterize changes in hydroclimatic dryness rather than to classify individual drought events by severity, the continuous PDSI values were retained for trend analysis without applying additional categorical drought thresholds.

Spatiotemporal Trend Analysis

Temporal trends in the monthly DFI and PDSI were independently evaluated for each pixel over the 2000–2024 study period using a combination of Sen's slope estimator and the Mann–Kendall (MK) significance test. This non-parametric approach was selected because it does not require the time series to follow a specific probability distribution and is widely used for assessing monotonic trends in environmental and hydroclimatic variables (Mann, 1945; Sen, 1968; Kendall, 1975). Sen's slope estimator was used to determine the magnitude and direction of temporal change, whereas the MK test was applied to assess whether the observed trend was statistically significant. The analysis was designed to characterize long-term monotonic trends using the conventional MK framework; no separate pre-whitening or autocorrelation correction was applied.

The same analytical procedure was applied independently to the DFI and PDSI time series at each spatial pixel. A significance level of $p < 0.05$ was adopted to distinguish statistically significant trends from non-significant changes. Based on the combination of trend direction and statistical significance, the pixels were classified into three categories: (*i*) significant increasing trend, (*ii*) significant decreasing trend, and (*iii*) non-significant trend. The latter category includes both positive and negative trends that did not reach the specified level of statistical significance. Accordingly, the trend analysis produced two spatially explicit three-class maps, one representing the long-term trend in dust occurrence and the other representing the long-term trend in drought conditions.

For DFI, a positive Sen's slope indicates an increasing frequency of dust occurrence, whereas a negative slope indicates a decreasing frequency. For PDSI, a negative trend indicates a shift toward drier conditions, while a positive trend indicates a shift toward wetter conditions. To facilitate consistent interpretation and direct comparison between the two hazards, PDSI trend directions were reoriented for spatial classification, so that increasing and decreasing trends represent increasing and decreasing drought conditions, respectively.

Integrated Drought–Dust Trend Analysis

The three-class trend maps of DFI and PDSI were integrated to identify areas characterized by different combinations of long-term drought and dust trends across Iran. The integration was performed through pixel-wise cross-classification of the two trend maps, whereby each pixel was assigned to one of the nine possible combinations derived from the three trend classes of each indicator: increasing, decreasing, and non-significant (Table 1). This approach provides a consistent framework for characterizing the spatial concurrence of changes in drought conditions and dust occurrence across Iran.

A decision matrix was developed to characterize the nine possible combinations of DFI and PDSI trend classes (Table 1). These combinations represent concurrent, contrasting, or non-significant trends between the two indicators. The resulting nine-class map was used to characterize and quantify the spatial distribution of different drought–dust trend configurations across Iran.

Although all nine combinations provide meaningful information on the spatial configuration of drought and dust trends, particular emphasis was placed on the classes in which both indicators exhibited significant trends. Among these, C1 represents the concurrent increase in dust occurrence and drought conditions, while C5 represents their concurrent decrease. C2 and C4 indicate contrasting trends between the two hazards. The remaining classes (C3, C6, C7, and C8) represent cases where only one indicator shows a significant trend, whereas C9 represents areas with no significant trend in either indicator (Table 1). All

Pre-publication Version

nine classes were retained to provide a complete representation of the spatial configurations of drought–dust trends across Iran.

Table 1. Decision matrix for the integrated classification of long-term dust and drought trends based on the three-class trend maps of DFI and PDSI across Iran.

Dust trend	Drought trend	Class	Integrated trend pattern
Increasing	Increasing	C1	Concurrent increase
Increasing	Decreasing	C2	Dust increase–drought decrease
Increasing	Non-significant	C3	Dust increase–no significant drought trend
Decreasing	Increasing	C4	Dust decrease–drought increase
Decreasing	Decreasing	C5	Concurrent decrease
Decreasing	Non-significant	C6	Dust decrease–no significant drought trend
Non-significant	Increasing	C7	No significant dust trend–drought increase
Non-significant	Decreasing	C8	No significant dust trend–drought decrease
Non-significant	Non-significant	C9	No significant trend in either indicator

Results and Discussion

Spatiotemporal Patterns of Dust Occurrence

The mean annual DFI distribution during 2000–2024 reveals pronounced heterogeneity in dust occurrence across Iran. in dust occurrence across Iran (Fig. 3a). The highest DFI values are primarily concentrated across southwestern, southern, and southeastern parts of the country, corresponding broadly to the major dust source regions identified from satellite observations (Fig. 2). Relatively high dust frequencies are also evident across parts of central Iran, including areas surrounding the Kavir Desert and Lut Desert, as well as in the vicinity of several major inland water bodies and dryland environments such as Hamoun Lakes and Jazmurian Depression. Elevated dust occurrence is additionally observed in parts of northwestern Iran, particularly around the Lake Urmia region. In contrast, northern and some northeastern areas generally exhibit lower frequencies of dusty conditions. This spatial variability reflects the combined influence of regional aridity, surface conditions, availability of exposed and erodible materials, vegetation cover, and atmospheric circulation and transport pathways (Papi et al., 2022). The concentration of high DFI values in southwestern Iran is also consistent with the influence of both domestic (Fig. 2) and transboundary dust sources across the Tigris–Euphrates region and neighboring drylands (Rashki et al., 2021).

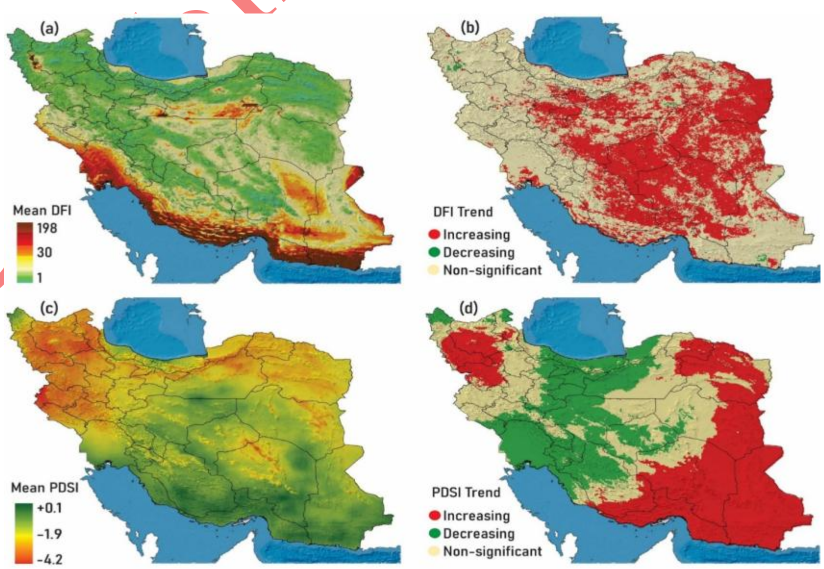

Fig 3. Spatial distribution of (a) mean annual Dust Frequency Indicator (DFI), (b) long-term trend in DFI, (c) mean Palmer Drought Severity Index (PDSI), and (d) long-term trend in drought conditions across Iran during 2000–2024. Trend classes are based on Sen’s slope and the Mann–Kendall test at the 0.05 significance level.

Pre-publication Version

The national-scale temporal evolution of annual DFI further indicates an overall increase in dust occurrence during 2000–2024 (Fig. 4a). Despite considerable interannual variability, the annual mean DFI shows a positive long-term tendency, indicating that the frequency of days meeting the adopted dust-occurrence threshold has generally increased over the study period. This increasing tendency becomes more evident in the latter part of the period, although substantial year-to-year fluctuations remain. Such variability is expected given the sensitivity of dust emission and atmospheric transport to short-term variations in precipitation, surface moisture, vegetation conditions, wind activity, and the availability of exposed sediment (Soleimani et al., 2026). Nevertheless, the overall positive linear trend suggests a broad increase in the recurrence of dusty conditions across Iran during the 25-year study period (Fig. 4a).
The observed increase in dust occurrence is particularly significant in the context of Iran's predominantly dry climate and the increasing hydroclimatic pressures affecting many parts of the country. Reduced moisture availability and degradation of vegetation and surface environments can increase the susceptibility of exposed soils and sediments to wind erosion, while variations in atmospheric circulation determine the activation and transport of dust (Darvishi Boloorani et al., 2026b). However, the positive national-scale tendency should not be interpreted as evidence of a uniform increase across the entire country. The marked spatial heterogeneity in mean DFI indicates that dust occurrence evolves differently across regions over the long term. Although the national average shown in Fig. 4 provides an overall temporal context for dust occurrence across Iran, it does not fully capture the substantial regional variability revealed by the pixel-level analysis. Therefore, pixel-level trend analysis is essential for identifying areas where dust activity has significantly increased, decreased, or remained relatively stable.
The spatial trend analysis reveals a predominantly increasing pattern in dust occurrence across Iran during 2000–2024 (Fig. 3b). Large areas of central Iran, together with extensive parts of the eastern and northeastern regions, experienced statistically significant increasing trends in DFI, indicating a long-term rise in the frequency of dusty conditions in these areas. In contrast, much of western and northwestern Iran, along with scattered areas in the north, northeast, southeast, and south, showed no statistically significant trend ($p > 0.05$). Decreasing trends accounted for only a small proportion of the national territory and were mainly concentrated around Lake Urmia, parts of the Kavir Desert in Semnan Province, and southern Sistan and Baluchestan. Overall, the spatial distribution of trend classes indicates that the long-term increase in dust occurrence is geographically heterogeneous rather than uniform across the country (Fig. 3b), and areas with high mean DFI do not necessarily exhibit the strongest increasing trends because mean DFI reflects the average level of dust occurrence, whereas the trend reflects its temporal change during the study period. The pixel-level trend analysis therefore provides a spatially explicit basis for distinguishing areas of significant change from those without statistically supported trends, enabling a more robust assessment of the spatial concurrence between dust occurrence and drought trends in the subsequent analysis.

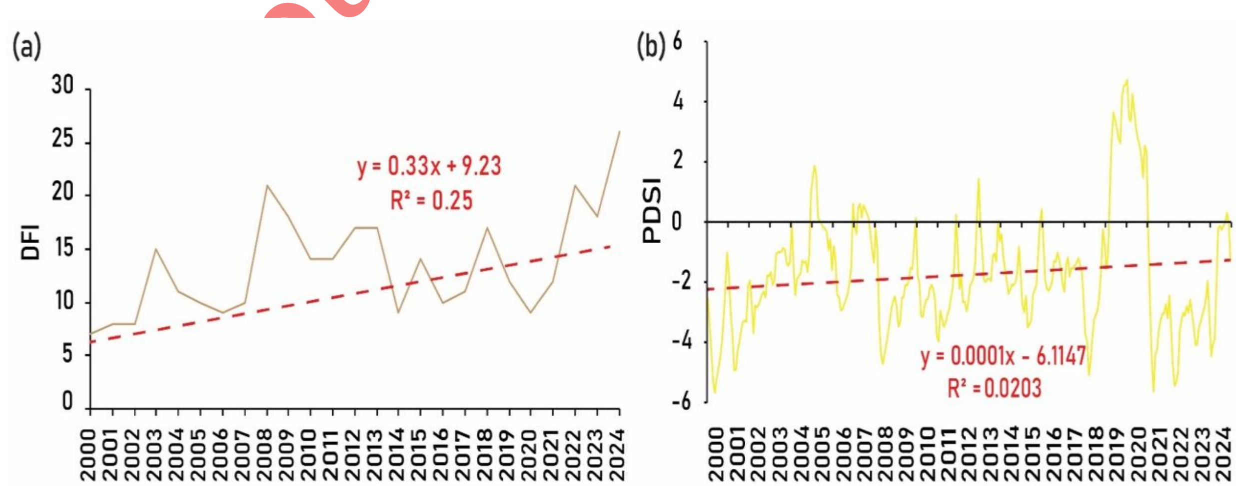

Fig 4. Interannual variations in (a) spatially averaged annual Dust Frequency Indicator (DFI) and (b) spatially averaged annual Palmer Drought Severity Index (PDSI) across Iran during 2000–2024.

Spatiotemporal Patterns of Drought Conditions

The spatial distribution of mean PDSI during 2000–2024 reveals pronounced heterogeneity in drought conditions across Iran (Fig. 3c). The strongest long-term drought conditions are concentrated in western and northwestern Iran, where mean PDSI values indicate persistent negative hydroclimatic conditions throughout the study period. The southern slopes of the Alborz Mountains, particularly across Tehran, Alborz, and Qazvin provinces, as well as parts of northeastern and eastern Iran, also experienced predominantly dry conditions, although with lower intensity than the western and northwestern regions. Across the country, mean PDSI values ranged from approximately −4.2 to +0.1, indicating a strong dominance of negative conditions in the spatial distribution of the index. It should be noted that these values represent averages over the entire 25-year period and therefore smooth the magnitude of individual drought episodes; substantially more severe conditions occurred during some individual months and years.

In contrast, much of central Iran, except for northern parts of Kerman Province, exhibited relatively weak drought conditions, with areas extending across the central drylands generally showing values close to neutral conditions. The southern and southeastern coastal regions also showed comparatively less severe drought conditions. In particular, southern and southeastern Iran exhibited relatively stronger positive PDSI signals, indicating periods of wetter-than-normal hydroclimatic conditions when averaged over the study period (Fig. 3c). Overall, the spatial distribution demonstrates that drought severity has not been spatially uniform across Iran, reflecting big regional differences in precipitation availability, temperature, evapotranspiration demand, topography, and broader atmospheric circulation.

The annual evolution of spatially averaged PDSI further highlights substantial interannual variability in hydroclimatic conditions during 2000–2024 (Fig. 4b). The early years of the period were characterized by predominantly negative annual mean values, with particularly dry conditions during 2000–2001. Hydroclimatic conditions gradually improved during 2002–2005, culminating in a near-neutral to slightly wet annual mean in 2005. This relatively favorable period was followed by renewed dry conditions during 2006 and 2008–2011. Moderate drought conditions persisted through much of 2012–2018, although their magnitude varied considerably among individual years.

A pronounced departure from this predominantly dry pattern occurred during 2019–2020, when the national mean PDSI shifted sharply toward positive values (Fig. 4b). Annual mean PDSI reached approximately 2.48 in 2019 and 3.03 in 2020, representing the most pronounced wet conditions in the study period. This wet episode was followed by an abrupt return to negative conditions in 2021–2023, with annual mean PDSI values of approximately −3.41, −3.76, and −3.13, respectively. Conditions partially recovered in 2024, although the annual mean PDSI remained negative (approximately −1.35). These strong year-to-year fluctuations demonstrate that national-scale drought conditions were characterized by alternating dry and wet episodes rather than a simple monotonic temporal trajectory.

The contrast between the spatially persistent drought patterns and the pronounced interannual variability is particularly important for interpreting the relationship between drought and dust occurrence. While the national mean series captures broad hydroclimatic fluctuations, it can mask substantial regional differences in the direction and magnitude of drought change. The spatial trend analysis therefore provides a more informative basis for identifying areas where drought conditions have significantly intensified or weakened during 2000–2024.

The spatial trend analysis of drought conditions (Fig. 3d) reveals a heterogeneous but relatively clustered pattern across Iran. Significant increasing trends in drought conditions are mainly concentrated along a broad northeast–southeast belt, extending across eastern and southeastern Iran, as well as in Hormozgan and southern and southeastern Fars. Sistan and Baluchestan and Hormozgan are almost entirely characterized by increasing drought trends. Another prominent cluster of increasing drought conditions occurs in northwestern Iran, particularly around the Lake Urmia region. In contrast, a distinct northeast–southwest-oriented belt is characterized predominantly by significant decreasing trends in drought conditions. This pattern includes Tehran and Qom, as well as substantial parts of Khuzestan and Kohgiluyeh and Boyer-Ahmad, where decreasing drought trends are spatially extensive.

Overall, the contrasting distribution of increasing and decreasing drought trends highlights big regional differences in the long-term evolution of hydroclimatic conditions across Iran. Increasing drought

Pre-publication version

conditions are particularly evident across parts of eastern, southeastern, and northwestern Iran, whereas decreasing drought trends form a relatively coherent zone across parts of central and southwestern Iran. This spatial heterogeneity provides an important context for interpreting the integrated drought–dust patterns, as areas with similar drought trends may exhibit markedly different responses in dust occurrence depending on their underlying climatic and environmental characteristics.

Comparison of the mean annual DFI (Fig. 3a) and mean PDSI (Fig. 3c) reveals a clear spatial mismatch between dust occurrence and drought conditions. The highest DFI values are concentrated mainly across southwestern to southeastern Iran, parts of central Iran, and around the Hamoun Lakes, with some areas experiencing more than 30 dusty days per year on average and locally reaching approximately 198 dusty days during 2000–2024. However, these regions generally show near-neutral to slightly positive mean PDSI values, indicating weakly dry to weakly wet average hydroclimatic conditions. This pattern reflects the distinction between hydroclimatic variability and the inherent susceptibility of dryland surfaces to dust emission. Many of the high-DFI areas are arid to hyper-arid environments characterized by sparse vegetation and exposed or sediment-rich surfaces that favor aeolian activity (Papi et al., 2022), allowing frequent dust occurrence even in the absence of pronounced mean drought conditions. Conversely, western and northwestern Iran exhibit stronger negative mean PDSI values but generally lower DFI, reflecting their relatively wetter and more topographically complex environments, where drought intensification does not necessarily result in high dust frequency. Overall, these contrasting spatial patterns indicate that dust occurrence is not controlled by drought intensity alone, but is conditioned by the background climatic regime, surface characteristics, vegetation, sediment availability, and atmospheric transport processes (Darvishi Boloorani et al., 2024c). Therefore, the drought–dust relationship should be assessed primarily through their temporal trends and local environmental context rather than inferred solely from their long-term mean spatial distributions.

Taken together, these results indicate that drought evolution across Iran is strongly spatially heterogeneous. The absence of a pronounced monotonic trend in the national-scale annual PDSI series does not imply an absence of long-term drought changes at the local scale. Rather, opposing regional trends can partially offset one another when aggregated across the country. The spatial trend map therefore provides an essential complement to the national temporal analysis and, importantly, establishes the spatially explicit drought trend layer required for comparison with the corresponding trends in dust occurrence.

Spatial Patterns of Concurrent Drought–Dust Trends

The integrated spatial classification of long-term drought and dust trends reveals a pronounced spatial heterogeneity in the concurrence of these two environmental hazards across Iran (Fig. 5). Among the nine possible trend combinations (Table 1), C7 (no significant dust trend–drought increase) represents the largest share of the country's area, accounting for approximately 24% of the total area. This class is predominantly distributed across northwestern, northeastern, eastern, and southeastern Iran. The dominance of C7 indicates that a considerable portion of the country has experienced a significant increase in drought conditions without a corresponding statistically significant long-term change in dust occurrence. This pattern further demonstrates that an intensification of drought does not necessarily translate into a significant increase in dust frequency at the national spatial scale, indicating that drought alone may not be a sufficient indicator of long-term changes in dust occurrence and that the response to hydroclimatic drying is strongly conditioned by local environmental and atmospheric factors. In contrast, C5 (concurrent decrease), representing areas where both drought and dust occurrence exhibit significant decreasing trends, constitutes the smallest share of the country, covering less than 1% of the total area. These areas are highly scattered and generally limited to only a few pixels, making them barely discernible at the national scale in Fig. 5. The very limited extent of C5 reflects the observed spatial pattern during 2000–2024, although its small area is also partly constrained by the significance criterion, which requires statistically significant decreasing trends in both drought and dust occurrence. Therefore, the results provide little evidence for widespread simultaneous decreases in both drought and dust occurrence across Iran during the study period. The very limited spatial extent of C5, compared with the considerably larger area occupied by concurrent

Pre-publication Version

increases (C1), suggests that simultaneous decreases in both hazards were not a widespread feature across Iran.
A particularly important pattern is represented by C1 (concurrent increase), which accounts for approximately 17% of Iran's total area. This class is concentrated predominantly in the northeastern, eastern, southeastern, and southern parts of the country, including extensive areas of North Khorasan, Razavi Khorasan, South Khorasan, Kerman, Sistan and Baluchestan, Hormozgan, southern and southeastern Fars, and southeastern Bushehr. Small and spatially isolated patches of C1 are also evident around Lake Urmia and in parts of Kurdistan. The C1 class identifies areas where increasing drought conditions and increasing dust occurrence have occurred simultaneously over the long term. The spatial concentration of this class in eastern and southeastern Iran is particularly noteworthy because these regions are among the country's most arid and hyper-arid environments, where sparse vegetation, exposed and erodible surfaces, and extensive aeolian sediment sources provide a high baseline susceptibility to dust emission (Darvishi Boloorani et al., 2026b).
The spatial concentration of C1 is broadly consistent with previously identified dust-prone regions in eastern and southeastern Iran, which have been recognized as important areas of dust generation and activity (Rashki et al., 2021; Darvishi Boloorani et al., 2026b). The occurrence of concurrent increases in these dryland environments suggests that increasing hydroclimatic stress may reinforce an already high inherent susceptibility to dust emission. In eastern Iran, dust activity is also strongly influenced by regional atmospheric circulation, particularly the Levar or "120-day" winds, which are prominent during spring and summer and contribute substantially to the occurrence and transport of dust events in southeastern Iran. The seasonal intensification of these winds has been associated with enhanced dust activity in the region (Alizadeh-Choobari et al., 2014, 2016). Moreover, dust generated from these source regions can affect areas beyond Iran, including Afghanistan, Pakistan, the United Arab Emirates, and Oman (Darvishi Boloorani et al., 2026b). Thus, the concentration of C1 across eastern and southeastern Iran highlights areas where increasing drought stress coincides spatially with environments that are naturally favorable for frequent dust emission and regional atmospheric transport. These interpretations are based on previously published evidence and provide contextual explanations for the observed spatial patterns; the effects of atmospheric circulation, land-surface conditions, and regional dust sources were not directly tested as explanatory variables in the present analysis.
The contrasting trend classes provide an additional perspective on the spatial relationship between drought and dust. In particular, C2 (dust increase–drought decrease) occupies a substantially larger area than C4 (dust decrease–drought increase). C2 is distributed mainly across central Iran, with additional areas occurring in Golestan, Tehran, Semnan, Qom, Bushehr, and Khuzestan. This pattern indicates that increasing dust occurrence is not necessarily associated with increasing drought conditions and, in several regions, has occurred despite a long-term decrease in drought conditions. Such contrasting behavior further supports the interpretation that dust dynamics are governed by a combination of factors rather than by drought alone (Soleimani et al., 2026). Changes in precipitation and soil moisture may influence surface erodibility, but vegetation dynamics, land degradation, sediment availability, wind regimes, and the activation or persistence of local and regional dust sources can modulate the response of dust occurrence independently of the long-term drought signal. These differences in environmental and atmospheric conditions may help explain why increasing dust occurrence can persist or emerge under decreasing drought conditions in C2, whereas the comparatively limited extent of C4 indicates that increasing drought conditions are less consistently accompanied by decreasing dust occurrence.
C4, representing decreasing dust occurrence concurrent with increasing drought conditions, is comparatively limited in spatial extent. Its much smaller contribution relative to C2 suggests that, across Iran, areas experiencing worsening drought conditions are more commonly characterized by either no significant change in dust occurrence (C7) or, in some regions, a simultaneous increase in dust occurrence (C1), rather than by a significant decline in dust activity. This asymmetry between C2 and C4 is important because it demonstrates that the relationship between the two hazards is not simply reciprocal: a reduction in drought conditions does not necessarily suppress dust occurrence, while increasing drought conditions do not uniformly produce increasing dust frequency.

Pre-publication Version

The remaining classes (C3, C6, C8, and C9) complement the principal spatial patterns by identifying areas where only one of the two variables exhibits a significant trend or where neither variable shows a statistically significant long-term change. Their inclusion provides a more complete representation of the spatial complexity of drought–dust interactions across Iran and prevents the national pattern from being interpreted solely in terms of concurrent changes. Overall, the integrated classification demonstrates that concurrent drought–dust trends are spatially localized rather than nationally uniform. The coexistence of C1, C7, and C2 as major spatial patterns indicates that the long-term evolution of dust occurrence cannot be explained by drought trends alone. Instead, the strength and direction of the dust response appear to depend on the interaction between hydroclimatic variability and the underlying climatic, geomorphological, land-surface, and atmospheric characteristics of each region.

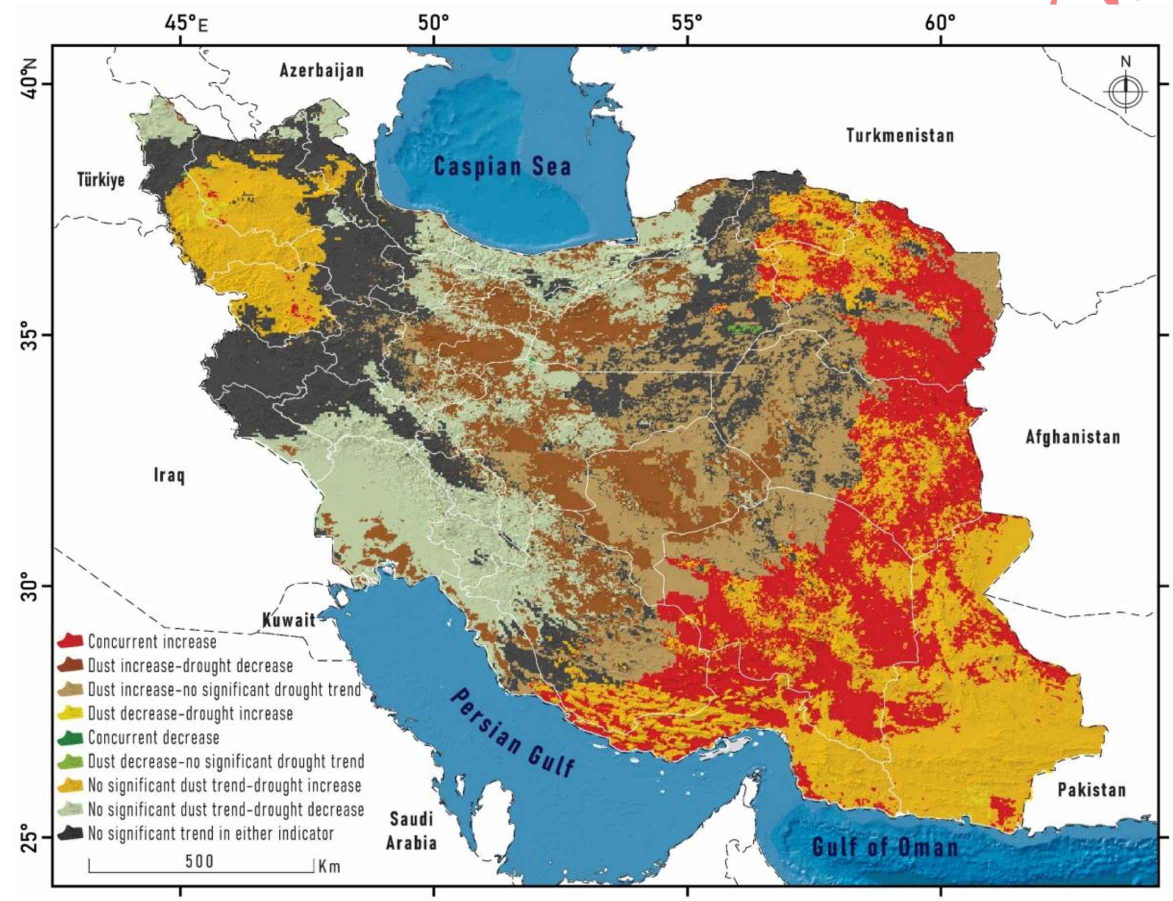

Fig 5. Spatial distribution of the nine integrated drought–dust trend classes across Iran during 2000–2024, based on the combination of long-term trends in Dust Frequency Indicator (DFI) and Palmer Drought Severity Index (PDSI).

Limitations and Interpretation of The Integrated Framework

Several considerations should be taken into account when interpreting the integrated drought–dust trend classes. First, the C1–C9 classification is based on the direction and statistical significance of the long-term trends rather than their magnitude. Consequently, areas assigned to the same class may still differ substantially in the strength of their underlying drought or dust trends. The classification is therefore intended to identify the spatial concurrence of significant trend directions rather than to quantify the magnitude of joint change.

Second, the analysis identifies spatial concurrence between long-term drought and dust trends but does not establish a direct causal relationship between the two variables. Dust occurrence is influenced by multiple

environmental and atmospheric factors, and the trend-based framework does not explicitly account for nonlinear responses, lagged effects, or short-term event-scale interactions. In addition, a single 2000–2024 trend may mask shorter-term variations or changes in the strength of the drought–dust association within the study period. These considerations should be taken into account when interpreting the spatial patterns identified in this study.
In addition, while the conventional MK framework provides a robust non-parametric approach for assessing long-term monotonic trends, potential temporal dependence in the time series should be considered when interpreting trend significance. Future studies could further evaluate this aspect using autocorrelation diagnostics and, where appropriate, autocorrelation-adjusted trend methods.

Implications For Climate-Related Environmental Change

The observed concurrence of drought and dust trends highlights broader patterns of climate-related environmental vulnerability across Iran's drylands. Regions characterized by concurrent increases in drought and dust occurrence may indicate areas of elevated environmental stress, particularly where hydroclimatic pressures coincide with persistent dust activity (Modarres, 2021; Khosroshahi et al., 2026). These patterns are relevant to ongoing climate-related environmental change because increasing climatic stress can have important implications for ecosystem stability, land degradation, and the resilience of dryland environments. However, the concurrent trends identified here should not be interpreted as evidence of a causal drought–dust relationship, but rather as an indication of regions where changes in drought conditions and dust occurrence evolve simultaneously. From an environmental management perspective, identifying such areas can support more integrated approaches to drought monitoring, land-degradation assessment, and dust-risk management under a changing climate.

Conclusion

This study provides an integrated assessment of the long-term spatiotemporal patterns of drought and dust occurrence across Iran during 2000–2024. Dust occurrence exhibited strong spatial heterogeneity but showed predominantly increasing trends across large parts of the country, while drought conditions displayed contrasting regional trends, with increasing drought conditions concentrated mainly in eastern and southeastern Iran. The integrated trend analysis revealed substantial spatial differences in the concurrence of these two hazards. Concurrent increases in drought and dust occurrence covered approximately 17% of Iran, whereas increasing drought accompanied by a non-significant dust trend constituted the largest integrated class, accounting for approximately 24% of the country. In contrast, concurrent decreases in both variables occupied less than 1% of the study area. These findings demonstrate that long-term trends in drought conditions and dust occurrence are spatially heterogeneous and that increasing drought does not necessarily coincide with a significant increase in dust occurrence. Rather than implying a direct causal relationship, the integrated classification identifies regions where the long-term trends of the two hazards occur concurrently or in contrasting directions. Overall, the proposed framework provides a spatially explicit basis for identifying areas of concurrent drought–dust trends and can support more targeted environmental monitoring, vulnerability assessment, and climate-change adaptation planning across Iran.

Acknowledgments

The authors used artificial intelligence (AI) tools only for language polishing, paraphrasing, and improving the clarity of the English language during the final stages of manuscript preparation. The authors take full responsibility for the content, scientific accuracy, interpretation, and conclusions presented in this manuscript.

References

Abatzoglou, J. T., Dobrowski, S. Z., Parks, S. A., & Hegewisch, K. C. (2018). TerraClimate, a high-resolution global dataset of monthly climate and climatic water balance from 1958–2015. *Scientific Data*, *5*(1), 170191. https://doi.org/10.1038/sdata.2017.191

Pre-publication Version

Ahrari, A., Panchanathan, A., & Haghighi, A. T. (2024). Dust over water: Analyzing the impact of lake desiccation on dust storms on the Iranian Plateau. *Journal of Hazardous Materials*, *480*, 136377. https://doi.org/10.1016/j.jhazmat.2024.136377
Al-Hemoud, A., Naghibi, A., Hashemi, H., Petrov, P., Kamal, H., Al-Senafi, A., ... & Darvishi Boloorani, A. (2024). Dust source susceptibility in the lower Mesopotamian floodplain of Iraq. *Remote Sensing Applications: Society and Environment*, *36*, 101355. https://doi.org/10.1016/j.rsase.2024.101355
Alizadeh-Choobari, O., Ghafarian, P., & Owlad, E. (2016). Temporal variations in the frequency and concentration of dust events over Iran based on surface observations. *International Journal of Climatology*, *36*(4), 2050–2062. https://doi.org/10.1002/joc.4479
Alizadeh-Choobari, O., Zawar-Reza, P., & Sturman, A. (2014). The "wind of 120 days" and dust storm activity over the Sistan Basin. *Atmospheric Research*, *143*, 328–341. https://doi.org/10.1016/j.atmosres.2014.02.001
Darvishi Boloorani, A., Nasiri, N., Papi, R., Soleimani, M., Neysani Samany, N., Al-Hemoud, A., ... & Al-Dousari, A. (2026a). Climate change has intensified drought in the Middle East over the last century. *Journal of Hydrology: Regional Studies*, *66*, 103612. https://doi.org/10.1016/j.ejrh.2026.103612
Darvishi Boloorani, A., Nasiri, N., Soleimani, M., Papi, R., Neysani Samany, N., Amiri, F., & Al-Hemoud, A. (2024b). Climate change, dust storms, and air pollution in the MENA region. In *Climate change and environmental degradation in the MENA region* (pp. 327-343). Cham: Springer Nature Switzerland. https://doi.org/10.1007/698_2024_1144
Darvishi Boloorani, A., Soleimani, M., Nasiri, N., Amiri, F., Neysani Samany, N., Al-Hemoud, A., ... & Huang, K. (2026b). Satellite-based assessment of dust storms originating from Eastern Iran with measurable transboundary impacts. *Atmospheric Research*, 109227. https://doi.org/10.1016/j.atmosres.2026.109227
Darvishi Boloorani, A., Soleimani, M., Neysani Samany, N., Papi, R., Nasiri, N., Amiri, F., ... & Al-Hemoud, A. (2024a). Climate change, drought, and water scarcity in the MENA region. In *Climate Change and Environmental Degradation in the MENA Region* (pp. 189- 204). Cham: Springer Nature Switzerland. https://doi.org/10.1007/698_2024_1143
Darvishi Boloorani, A., Soleimani, M., Papi, R., Nasiri, N., Neysani Samany, N., Mirzaei, S., & Al-Hemoud, A. (2024c). Assessing the role of drought in dust storm formation in the Tigris and Euphrates basin. *Science of The Total Environment*, *921*, 171193. https://doi.org/10.1016/j.scitotenv.2024.171193
Eskandari Dameneh, H., Gholami, H., Telfer, M. W., Comino, J. R., Collins, A. L., & Jansen, J. D. (2021). Desertification of Iran in the early twenty-first century: assessment using climate and vegetation indices. *Scientific Reports*, 11(1), 20548. https://doi.org/10.1038/s41598-021-99636-8
Fakhar, M. S., & Nazari, B. (2024). Monitoring and Assessing Spatial and Temporal Characteristics of Drought in Iran Using Remote Sensing. *Journal of Drought and Climate Change Research (JDCR)*, *2*(1), 39-58. https://doi.org/10.22077/jdcr.2024.7011.1050 [In Persian]
Ginoux, P., Prospero, J. M., Gill, T. E., Hsu, N. C., & Zhao, M. (2012). Global-scale attribution of anthropogenic and natural dust sources and their emission rates based on MODIS Deep Blue aerosol products. *Reviews of Geophysics*, *50*(3), RG3005. https://doi.org/10.1029/2012RG000388
Intergovernmental Panel on Climate Change. (2023). Deserts, semiarid areas and desertification. In H.-O. Pörtner, D. C. Roberts, M. Tignor, E. S. Poloczanska, K. Mintenbeck, A. Alegría, M. Craig, S. Langsdorf, V. Möller, A. Okem, & B. Rama (Eds.), Climate change 2022: Impacts, adaptation and vulnerability: Contribution of Working Group II to the Sixth Assessment Report of the Intergovernmental Panel on Climate Change (pp. 2195–2232). *Cambridge University Press*. https://doi.org/10.1017/9781009325844.020
Kendall, M. G. (1975). Rank correlation methods (4th ed.). *Charles Griffin & Company Ltd*. https://search.worldcat.org/title/Rank-correlation-methods/oclc/136868
Khosroshahi, M., Ebrahimi-Khusfi, Z., & Saeedifar, Z. (2026). Nonlinear environmental controls and threshold effects on dust events in Iran's arid and semi-arid regions. *Scientific Reports, 16*, 19473. https://doi.org/10.1038/s41598-026-50623-x
Lyapustin, A., Wang, Y., Korkin, S., & Huang, D. (2018). MODIS Collection 6 MAIAC algorithm. *Atmospheric Measurement Techniques*, *11*(10), 5741-5765. https://doi.org/10.5194/amt-11-5741-2018
Mahdizadeh, J., Ghavidel, Y., & Farajzadeh, M. (2025). High-resolution spatiotemporal analysis of drought dynamics in Iran. *Environmental Monitoring and Assessment*, *197*(9), 1005. https://doi.org/10.1007/s10661-025-14443-2
MalAmiri, N., Rashki, A., Al-Dousari, A., & Kaskaoutis, D. G. (2025). Socioeconomic and health impacts of dust storms in Southwest Iran. *Atmosphere*, *16*(2), 159. https://doi.org/10.3390/atmos16020159
Mann, H. B. (1945). Nonparametric tests against trend. *Econometrica, 13*(3), 245-259. https://doi.org/10.2307/1907187
Mesgaran, M., Madani, K., Hashemi, H., & Azadi, P. (2016). Evaluation of land and precipitation for agriculture in Iran. *Stanford Iran*, *2040*. https://purl.stanford.edu/vf990qz0340

Prepublication Version

Modarres, R. (2021). Dust storm frequency change in relation to climate drivers. *International Journal of Climatology*, *41*, E187-E199. https://doi.org/10.1002/joc.6675
Neira, M., Erguler, K., Ahmady-Birgani, H., Al-Hmoud, N. D., Fears, R., Gogos, C., ... & Christophides, G. (2023). Climate change and human health in the Eastern Mediterranean and Middle East: Literature review, research priorities and policy suggestions. *Environmental Research*, *216*, 114537. https://doi.org/10.1016/j.envres.2022.114537
Papi, R., Kakroodi, A. A., Soleimani, M., Karami, L., Amiri, F., & Alavipanah, S. K. (2022). Identifying sand and dust storm sources using spatial-temporal analysis of remote sensing data in Central Iran. *Ecological Informatics*, *70*, 101724. https://doi.org/10.1016/j.ecoinf.2022.101724
Pato, M., Moradi, S., & Henareh, J. (2025). Investigating the effects of climate change and dust storms on the health and sustainability of the Zagros forest ecosystem. *Journal of Drought and Climate Change Research (JDCR), 3* (Special Issue), 1- 16. https://doi.org/10.22077/jdcr.2025.9043.1126 [In Persian]
Pouyan, S., Bordbar, M., Ravichandran, V., Tiefenbacher, J. P., Kherad, M., & Pourghasemi, H. R. (2023). Spatiotemporal monitoring of droughts in Iran using remote-sensing indices. *Natural Hazards*, *117*(1), 1-24. https://doi.org/10.1007/s11069-023-05847-9
Rahnama, S., Shahidi, A., Yaghoobzadeh, M., & Mehran, A. A. (2024). Comparison of different drought monitoring indices in different climatic conditions in Iran. *Atmósfera*, *38*. https://doi.org/10.20937/atm.53319
Rashki, A., Middleton, N. J., & Goudie, A. S. (2021). Dust storms in Iran–Distribution, causes, frequencies, and impacts. *Aeolian Research*, *48*, 100655. https://doi.org/10.1016/j.aeolia.2020.100655
Sen, P. K. (1968). Estimates of the Regression Coefficient Based on Kendall's Tau. *Journal of the American Statistical Association*, *63*(324), 1379–1389. https://doi.org/10.1080/01621459.1968.10480934
Shi, L., Zhang, J., Yao, F., Zhang, D., & Guo, H. (2021). Drivers of dust emissions over the dust belt from 1980 to 2018 and their variation in two global warming phases. *Science of The Total Environment*, *767*, 144860. https://doi.org/10.1016/j.scitotenv.2020.144860
Soleimani, M., Argany, M., Papi, R., & Amiri, F. (2021). Satellite aerosol optical depth prediction using data mining of climate parameters. *Physical Geography Research*, *53*(3), 319-333. https://doi.org/10.22059/jphgr.2021.318600.1007591 [In Persian]
Soleimani, M., Darvishi Boloorani, A., Neysani Samany, N., Ghayamghamian, M. R., & Al-Hemoud, A. (2026). Assessment of dust storm hazardousness in Iran using remotely sensed aerosol loading and hydroclimatic data. *Remote Sensing Applications: Society and Environment*, 102033. https://doi.org/10.1016/j.rsase.2026.102033
Sotoudeheian, S., Salim, R., & Arhami, M. (2016). Impact of Middle Eastern dust sources on PM10 in Iran: Highlighting the impact of Tigris-Euphrates basin sources and Lake Urmia desiccation. *Journal of Geophysical Research: Atmospheres*, *121*(23), 14,018–14,034. https://doi.org/10.1002/2016JD025119
Tosan, M., Shamshirgaran, R., & Falaki, M. (2025). A Review of Participatory Management's Role in Reducing Vulnerability and Enhancing Resilience to Climate Change and Drought (2006-2024). *Journal of Drought and Climate Change Research (JDCR), 2*(8), 161-184. https://doi.org/10.22077/jdcr.2025.8565.1095
Vaghefi, S. A., Keykhai, M., Jahanbakhshi, F., Sheikholeslami, J., Ahmadi, A., Yang, H., & Abbaspour, K. C. (2019). The future of extreme climate in Iran. *Scientific Reports*, 9(1), 1464. https://doi.org/10.1038/s41598-018-38071-8
Yu, Y., Notaro, M., Kalashnikova, O. V., & Garay, M. J. (2016). Climatology of summer Shamal wind in the Middle East. *Journal of Geophysical Research: Atmospheres*, *121*(1), 289-305. https://doi.org/10.1002/2015JD024063
Zittis, G., Almazroui, M., Alpert, P., Ciais, P., Cramer, W., Dahdal, Y., ... & Lelieveld, J. (2022). Climate change and weather extremes in the Eastern Mediterranean and Middle East. *Reviews of Geophysics*, *60*(3), e2021RG000762. https://doi.org/10.1029/2021RG000762

Pre-publication Version